Science of the Total Environment 622–623 (2018) 1016–1028

Contents lists available at ScienceDirect

Science of the Total Environment

journal homepage: www.elsevier.com/locate/scitotenv

Comparison of baseline period choices for separating climate and land use/land cover change impacts on watershed hydrology using distributed hydrological models

Ling Zhang [a], Zhuotong Nan [b,c,*], Wenjun Yu [d], Yanbo Zhao [a], Yi Xu [b,c]

[a] Key Laboratory of Remote Sensing of Gansu Province, Northwest Institute of Eco-Environment and Resources, Chinese Academy of Sciences, Lanzhou 730000, China
[b] Ministry of Education Key Laboratory of Virtual Geographic Environment, Nanjing Normal University, Nanjing 210023, China
[c] Jiangsu Center for Collaborative Innovation in Geographical Information Resource Development and Application, Nanjing 210023, China
[d] College of Hydrometeorology, Nanjing University of Information Science & Technology, Nanjing 210023, China

HIGHLIGHTS

- Two hydrological models were applied to compare baseline period choices for separating hydrological impacts.
- Real and hypothetical LUCC cases were used to test the influences of baseline period choices.
- Contributions of LUCC and climate change vary noticeably between various baseline period choices.
- Influences of baseline period choices can diverge significantly between different hydrological models.
- Some useful recommendations regarding baseline period selection have been proposed.

GRAPHICAL ABSTRACT

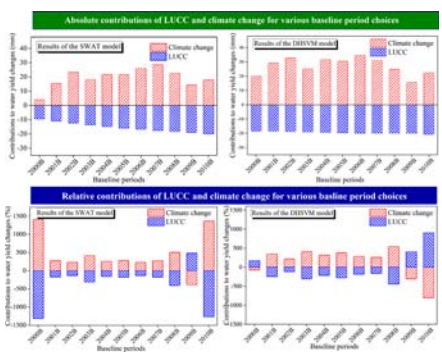

ARTICLE INFO

Article history:
Received 26 September 2017
Received in revised form 19 November 2017
Accepted 5 December 2017
Available online xxxx

Editor: Ouyang Wei

Keywords:
Hydrological impact
Baseline period choice
Climate change
Land use/land cover
Hydrological model

ABSTRACT

Separating impacts of land use/land cover change (LUCC) and climate change on hydrology is essential for watershed planning and management. This is typically done via hydrological modelling in combination with the one-factor-at-a-time analysis. However, it remains unclear how large the differences in isolated hydrological impacts would be when selecting different baseline periods. In this study, we compared baseline period choices for separating climate change and LUCC impacts on watershed hydrology in a typical inland river basin in northwest China, i.e. the Upper Heihe River Basin, with two hydrological models, i.e., Soil and Water Assessment Tool and Distributed Hydrology Soil Vegetation Model. In the real LUCC case which considers the actual land use changes between 2000 and 2011, the absolute contributions of LUCC to the variations in water yield and ET are slight and almost have the same magnitude for different baseline period choices, whereas those of climate change are substantial and with varying magnitudes. Compared with the absolute contributions, the relative contributions of climate change and LUCC seem less sensitive to the choices of baseline periods. In the hypothetical LUCC case which assumes an extreme land use conversion (i.e., grassland converts to farmland completely), both climate change and LUCC contribute to the changes in water yield and ET significantly. Moreover, both the absolute and relative contributions diverge noticeably between various baseline period choices. The influences of baseline period choices on the partitioning of hydrological impacts diverge significantly between different hydrological models.

* Corresponding author at: Ministry of Education Key Laboratory of Virtual Geographic Environment, Nanjing Normal University, Nanjing 210023, China.
E-mail address: nanzt@njnu.edu.cn (Z. Nan).

https://doi.org/10.1016/j.scitotenv.2017.12.055

This study highlights that baseline period choice is an important source of uncertainty when disentangling the impacts of LUCC and climate change on hydrology. Some useful recommendations regarding baseline period selection have been proposed, which may help to reduce the uncertainties associated with baseline period choices.

1. Introduction

Land use/land cover change (LUCC) and climate change are two of the most important drivers of hydrological variations (Tu, 2009; Khoi and Suetsugi, 2014; Kundu et al., 2017; Trang et al., 2017). LUCC can affect hydrological processes such as evapotranspiration (ET), interception, infiltration and surface runoff by directly altering morphological and physiological conditions of the landscape, and by indirectly modifying soil and atmospheric boundary layers (Molina-Navarro et al., 2014; Cuo, 2016). Meanwhile, climate change, particular the shifts in precipitation and temperature, can also exert a profound impact on hydrological conditions and spatial-temporal patterns of water resources (Pechlivanidis et al., 2016; Sorribas et al., 2016; Sunde et al., 2017). The impact assessments of LUCC and climate change have garnered considerable attentions from the scientific community as well as decision and policy makers in the context of increasing water scarcity (Wang et al., 2013; Gao et al., 2016; Wagner et al., 2017).

LUCC and climate change generally intertwine together in their impacts on hydrological regimes (Kim et al., 2013; Zhang et al., 2016). Some preceding studies have investigated the combined hydrological influences of LUCC and climate change (e.g. Choi, 2008; Franczyk and Chang, 2009; Qi et al., 2009; Tu, 2009; Zhang et al., 2015). These investigations are able to provide useful information for watershed planning and management. Nevertheless, the individual contributions of LUCC and climate change have not been determined sufficiently due to the existence of nonlinearity in hydrological behaviors (Wang et al., 2013; Dey and Mishra, 2017). In order to better manage our watersheds, it is vital to figure out not only the joint influence of LUCC and climate change, but also their individual and relative contributions (Wang et al., 2013; Zhang et al., 2016).

Various methods have been proposed and utilized to disentangle LUCC and climate change impacts on watershed hydrology (Gao et al., 2016; Dey and Mishra, 2017). They can be grouped into following categories: (i) hydrological modelling approach (Yin et al., 2017; Zhang et al., 2017); (ii) paired catchment approach (Bosch and Hewlett, 1982; Brown et al., 2005; McCormick et al., 2009); (iii) conceptual approach (e.g. the Budyko framework (Gao et al., 2016) and Tomer Schilling framework (Tomer and Schilling, 2009)); (iv) empirically statistical method (Zhang et al., 2008; Wei and Zhang, 2010); and (v) analytical approach (e.g. climate elasticity method (Zheng et al., 2009) and hydrological sensitivity method (Li et al., 2012)). With increasing data availability and rapid development of process-based distributed hydrological models, the hydrological modelling approach, which is usually combined with one-factor-at-a-time (OFAT) analysis, has gradually become one of the most widely-used methods for isolating hydrological impacts of LUCC from those of climate change (e.g. Li et al., 2009; Shi et al., 2013; Natkhin et al., 2015; Guo et al., 2016; Luo et al., 2016; Yan et al., 2016; Zhang et al., 2016; Zuo et al., 2016; Setyorini et al., 2017; Yang et al., 2017; Yin et al., 2017; Zhang et al., 2017).

The hydrological modelling approach typically consists of three steps (i) calibrating and validating the selected hydrological model for the target region; (ii) designing and performing OFAT modelling experiments; and (iii) finally comparing the simulated results of different experiments. The determination of baseline period from the entire study time span is essential in the process of designing OFAT experiments. Currently, however, there is actually not a general rule of thumb applicable to the selection of baseline period. Mostly, the entire study period is split into two equal time-slices, of which the first one is selected as the baseline period (e.g. Li et al., 2009; Niraula et al., 2015; Zhang et al., 2016; Zhang et al., 2017). In some other cases, the length of baseline period is determined to be obviously longer than that of the comparative one (e.g. Shi et al., 2013; Yin et al., 2017). Additionally, in very few cases, the baseline period was selected based on the detecting results of the temporal trends and abrupt change points of hydrological variables such as streamflow (Zuo et al., 2016). Various baseline period choices may bring biases to the distinguished impacts of LUCC and climate variability on hydrology. However, to our knowledge, no previous studies have reported the range of diversity when choosing different baseline periods, which constitutes the most important motivation behind this study.

In recent years, a few studies have assessed the differences in the estimated hydrological variations due to LUCC or climate change resulting from the use of different models (e.g. Jiang et al., 2007; Chen et al., 2012; Cornelissen et al., 2013; Morán Tejeda et al., 2015; Karlsson et al., 2016). They reported that model choices could exert a significant influence on hydrological impact assessments. This seems quite obvious, considering that hydrological models generally differ in their structures, complexities and process presentations (Morán Tejeda et al., 2015). However, it is often omitted in most previous studies that were carried out with only one model (e.g. Baker and Miller, 2013; Kim et al., 2013; Zhou et al., 2013; Bieger et al., 2015).

Therefore, in this study, our primary goal is to compare baseline period choices for separating impacts of LUCC and climate change on watershed hydrology. The goal was implemented through the applications of two distributed hydrological models, i.e., the Soil and Water Assessment Tool (SWAT) and Distributed Hydrology Soil Vegetation Model (DHSVM), together with eleven baseline periods, to a typical inland river basin in northwest China (i.e., the upper Heihe River Basin). Specifically, we aim to address the following questions: (i) how large would be the differences in the isolated hydrological impacts when choosing different baseline periods? (ii) how large would be the divergence of the influences of baseline period choices when using different hydrological models? and (iii) what can be done to reduce the uncertainties associated with baseline period choice?

2. Materials and methods

2.1. Study area and data

2.1.1. Study area

The Heihe River Basin (HRB) is the second largest inland river basin in China. It is located in a transitional zone between semiarid and arid areas (Tian et al., 2015). The basin serves as a typical study region in China for exploring the interactions between ecology, water and economy owing to the distinct landscape patterns, special eco-hydrological processes and serious water problems (Zhang et al., 2016). The upper HRB (hereafter referred to as UHRB) has a drainage area of approximately 10,000 km^2, and is studied in this research (Fig. 1). It is the main headwater region of the Heihe River and plays an essential role in supporting agricultural developments in the middle stream region and maintaining healthy ecological systems in the lower stream region (Zhang et al., 2016; Cong et al., 2017). The UHRB is characterized by mountainous topography, and has elevations ranging from 1408 m above sea level (ASL) in the mountain valley to 5228 m ASL at the mountain peak. The UHRB has a continental alpine semi-humid climate with an average precipitation of about 450 mm/year and a mean annual

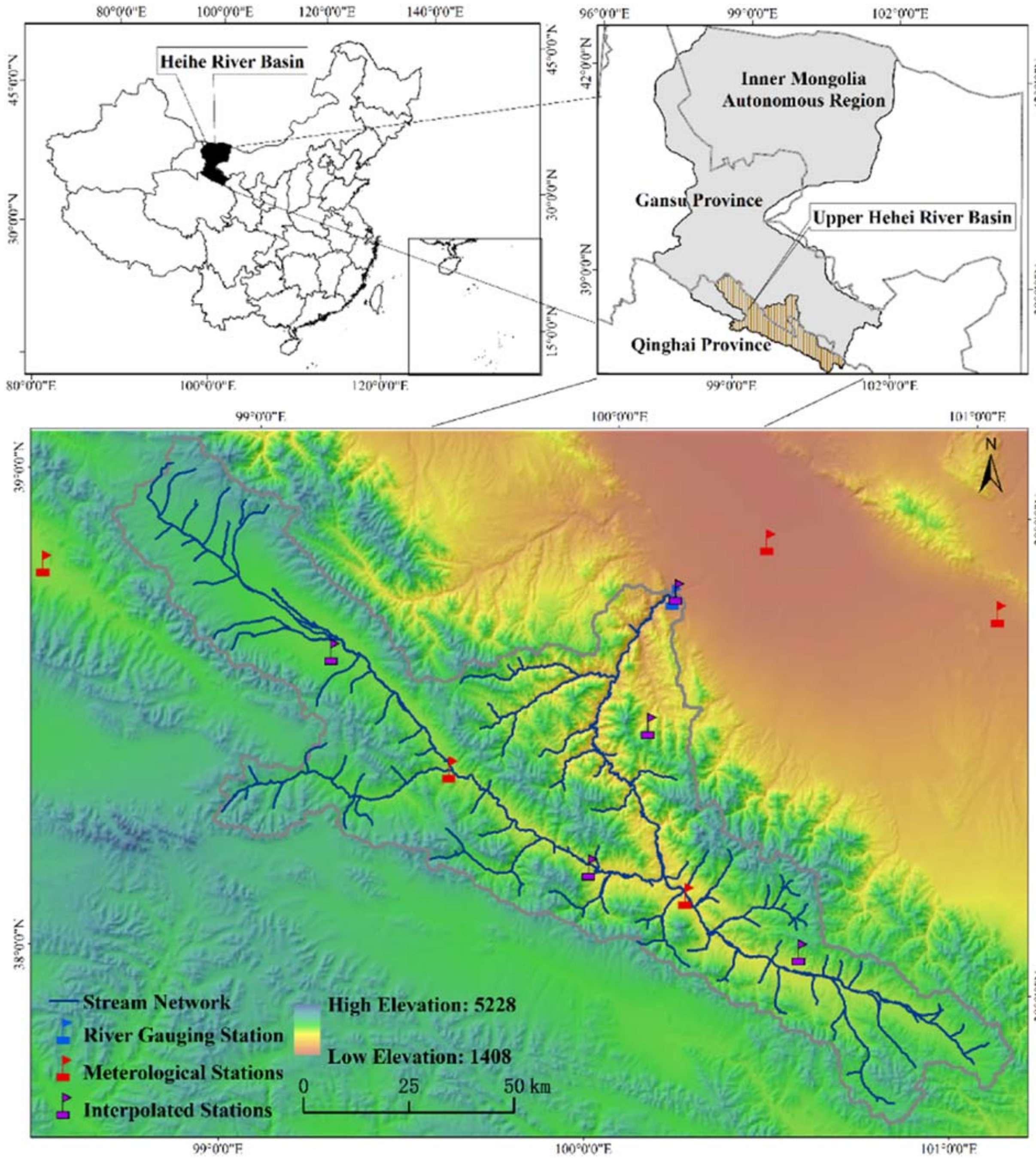

Fig. 1. Location map showing the topography of the study area and the hydro-meteorological stations.

temperature <1 °C from 1960 to 2014. Most of the precipitation (>90%) occurs in May to September while <5% in the winter months of December, January and February. The discharge from the UHRB shows strong seasonality, with an average value of about 16.05 × 10^8 m^3/year (Zhang et al., 2015). Snowfall is an important component of precipitation, and it contributes to spring streamflow significantly (Wang et al., 2015). The snowline is about 4500–4500 m ASL and increases from east to west (Dang et al., 2012). The snow is unevenly distributed in terms of space and time, owing to complex terrain and climatic system. The snow cover is mainly located in in the valleys with shady slope, and its area reaches the maximum in May and October, while the minimum in July (Hao et al., 2009; Dang et al., 2012). The land use/cover map of the year 2011, which was derived from the 30-m Landsat TM/ETM+ images, shows that the UHRB is mainly covered by grassland (69.2%) and barren land (24.2%) (Wang et al., 2014). The alpine meadow soil, alpine chestnut soil, subalpine shrub meadow soil and alpine frost desert soil are the dominant soil types in the UHRB (Yu et al., 2013); and the soil textures are mainly loam, silt loam and sandy loam (Lu et al., 2011).

2.1.2. Data

The dataset used in this study include: (i) digital elevation model (DEM); (ii) land use map; (iii) soil map and properties; and (iv) hydro-meteorological data. The 90-m DEM in the study area has been subset and resampled from the original ASTER Global DEM at a 30-m resolution. The land use maps at a scale of 1: 100,000 were collected from the Science Data Center for Cold and Arid Regions (SCAR, http://westdc.westgis.ac.cn). The land use/cover datasets in 2000 and 2011 were derived from the Landsat TM/ETM+ satellite images through visual interpretation and have high classification accuracy (Wang et al., 2014; Wang et al., 2014; Hu et al., 2015). All the land use/cover datasets were produced using the two-level hierarchical classification system that includes 6 first-level and 26 second-level classes. In this study, the second level classes were all reclassified into the first level classes, which consist of farmland, forest, grassland, water body, built-up land and barren land. The soil type map at the scale of 1:1,000,000 was subset from the second State Soil Survey of China (the latest nation-wide soil survey in China) completed in the early 1980s. The physical properties of each soil type such as texture, soil depth, saturated hydraulic conductivity and bulk density were partly obtained from Gansu Soil Handbook and partly from field observations as described by Yu et al. (2013) and Lai et al. (2013). All the spatial data were converted into a consistent grid format at a resolution of 300 m. Daily streamflow observations from 1994 to 2009 at the outlet of the UHRB, i.e., the Yingluoxia hydrological station, were also obtained from SCAR. Daily meteorological forcing data from 1960 to 2014, including maximum and minimum temperature, precipitation, relative humidity and wind speed measured at four national weather stations, were obtained from the China Meteorological Data Sharing Service System (http://cdc.nmic.cn/). Besides, the precipitation time series of five fictitious stations (Fig. 1) were interpolated through an intermediate-complexity, quasi-physically based meteorological model, i.e. MicroMet (Liston and Elder, 2006), in order to better capture the strong spatial heterogeneity of precipitation over the UHRB.

2.2. Hydrological models

The SWAT and DHSVM models were used in this study to investigate the influence of baseline period choices on the separation of hydrological impacts. They were selected mainly because of their free availability and wide applications for assessing hydrological impacts (e.g. Cuo et al., 2009; Li et al., 2009; Baker and Miller, 2013; Dickerson-Lange and Mitchell, 2014; Alvarenga et al., 2016; Zhang et al., 2017). The type, structure, spatial discretization and process representation of the two models are presented in Table 1.

2.2.1. SWAT

SWAT is a semi-distributed HRU-based eco-hydrological model (Arnold et al., 1998). It was developed to simulate and predict the impacts of land management practices on water, sediment and agricultural chemical yields in large complex watersheds with varying soils, land use and management conditions over long time periods (Neitsch et al., 2011). The SWAT model divides a watershed into sub-basins and further subdivides each sub-basin into a number of hydrological response units (HRUs), each of which represents a unique combination of land use, soil type and terrain slope. Taking HRU as the basic unit, hydrological components, nutrients and sediment yield are simulated and aggregated for each sub-basin, and then routed to the basin outlet throughout the channel network. Further details on SWAT can be found in Neitsch et al. (2011).

Table 1
Comparison of the SWAT and DHSVM models.

	SWAT	DHSVM
Model type	Semi-distributed	Fully-distributed
Spatial discretization	Hydrological response units (HRUs)	Regular grids
Interception	Storage approach; function of LAI	Storage approach; function of fractional coverage
Potential/actual evapotranspiration	Penman-Monteith or Priestley-Taylor or Hargreaves approach/reduction of PET by soil water content	Penman–Monteith approach/dependence on PET and water availability in root zone
Runoff components	Surface runoff, interflow and baseflow	Surface runoff and saturated subsurface flow
Surface runoff	SCS curve number or Green & Ampt infiltration method	Infiltration and saturation excess mechanism
Percolation	Storage routing method	Darcy's Law
Snow melt	Degree-day method	Mass and energy balance model
Routing methods	Kinematic storage model (interflow); linear storage approach (baseflow); variable storage method or Muskingum routing method (streamflow)	Kinematic wave model or cell-by-cell approach (overland flow); cell-by-cell approach (subsurface flow); linear storage method (streamflow)

2.2.2. DHSVM

DHSVM is a fully-distributed and grid-based hydrological model that was developed by the University of Washington (UW) and the Pacific Northwest National Laboratory (PNNL) in the early 1990s (Wigmosta et al., 1994). It was predominantly designed for mountainous regions with complex terrain, and can provide an integrated and dynamic representation of the distributions of snow cover, soil moisture, evapotranspiration and runoff at the spatial scale described by the DEM data. DHSVM divides a watershed into computational grid cells, each of which is assigned with surface cover and soil properties. Based on grid cells, the hydrological processes including ET, sow accumulation/melt, soil water movement, lateral saturated subsurface flow, overland flow and channel flow are simulated (Table 1). The DHSVM model has evolved rapidly over the past few decades. The most recently released version of the model is 3.1.2. Further details on DHSVM were documented in Wigmosta et al. (1994), Storck et al. (1998) and Wigmosta and Perkins (2001).

2.3. Model setup and calibration

2.3.1. Model setup

The SWAT and DHSVM models were applied to the UHRB using input and methods as similar as possible to ensure the divergence in the separated impacts of LUCC and climate change is due to model difference. Nevertheless, some typical ways that a model user would adopt to set up the individual model were still maintained to preserve the influence of a stand-alone model choice (Karlsson et al., 2016). For example, the climatic forcing data at a daily time step are usually prepared for SWAT, whereas those at a sub-daily time step are typically prepared for DHSVM. For another instance, the stream network and the related properties required by SWAT are typically generated using the tool of automatic watershed delineation within ArcSWAT, whereas those required by DHSVM are generally produced using an ArcInfo Macro Language (AML) script coming with the model.

The SWAT model was set up following our previous work (Zhang et al., 2016). The UHRB was delineated into 24 subbasins based on the 300 m DEM with a threshold area of 20,000 ha. The subbasins were further discretized to 143 HRUs by setting land use and soil threshold levels to 5% and 10%, respectively. The agricultural management was parameterized using the SWAT default values, owing to a very small proportion of agricultural lands (<1%) in the UHRB. The Penman-Monteith method was chosen to estimate potential evapotranspiration, the soil conservation service curve number (SCS-CN) method to compute surface runoff and the variable storage method to route channel flow.

For DHSVM, the size of the grid cells was set as 300 by 300 m to ensure an acceptable computational efficiency and, more importantly, to maintain consistency with the SWAT model in the process of watershed delineation. We employed the macroscale Variable Infiltration Capacity (VIC) model (Liang et al., 1994) to disaggregate daily meteorological observations to a 3-hourly time step, in the same manner as did in other studies (e.g. Thanapakpawin et al., 2007; Livneh et al., 2013; Voisin et al., 2013), in order to meet the general requirement of DHSVM. The Cressman scheme was selected to interpolate meteorological variables across the basin, the water table gradient to calculate lateral subsurface flow, and the cell-by-cell conventional approach to route overland flow. The root zone of the soil profile was divided into three layers, i.e., 0–10 cm, 10–35 cm and 35–75 cm. In line with the SWAT model, the precipitation and temperature lapse rates, which were estimated by Li (2012) using station records from 2000 to 2009, were set to 82 mm/km and −5 °C/km, respectively. The other constant parameters including rain leaf area index (LAI) multiplier, reference height and roughness of soil surface were set to 0.0005, 25 m and 0.02 m, respectively. The stream map and network, and the initial spatial pattern of soil depth were generated using the AML script available at the model's official site (http://dhsvm.pnnl.gov/).

2.3.2. Model calibration and evaluation

Both the SWAT and DHSVM models were calibrated manually against streamflow observations at the basin outlet. The sensitive parameters were optimized through a "trial and error" process; each parameter was adjusted at a time within its physically meaningful ranges. For SWAT, the sensitive parameters were primarily identified from the previous studies conducted in the UHRB (Li et al., 2009b; Lai et al., 2013; Yu et al., 2013; Wu et al., 2014; Wu et al., 2015). The descriptions, and initial and optimal values of those parameters are referred to Zhang et al. (2016). For DHSVM, the potential sensitive parameters were first identified from the previous works that were carried out in the other river basins (Cuo et al., 2006; Thanapakpawin et al., 2007; Cuo et al., 2009; Cuartas et al., 2012; Du et al., 2014; Alvarenga et al., 2016). Then, the most sensitive parameters were obtained for the UHRB through the one-at-a-time sensitivity analysis, which include total soil depth, lateral saturated hydraulic conductivity, exponential decrease rate of lateral saturated hydraulic conductivity, leaf area index (LAI), rain LAI multiplier, minimum/maximum stomatal resistance and rain/snow thresholds (minimum temperature at which rain/snow occurs). To mitigate the effects of inaccurate initial conditions, the climatic forcings for three years (1991–1993) were used to spin-up both the SWAT and DHSVM models. The years 1994 through 2001, and 2002 through 2009 were selected as the calibration and validation periods, respectively. The model performances were evaluated via visual hydrograph inspection and three statistical indices recommended by Moriasi et al. (2007), i.e., (i) Nash-Sutcliffe efficiency (NSE) (Nash and Sutcliffe, 1970), (ii) percent bias (PBIAS), and (iii) RMSE-observations standard deviation ratio (RSR). The equations for NSE, PBIAS and RSR are as follows.

$$\mathrm{NSE} = 1 - \frac{\sum_{i=1}^{n}\left(Q_i^{obs} - Q_i^{sim}\right)^2}{\sum_{i=1}^{n}\left(Q_i^{obs} - Q_{mean}^{obs}\right)^2} \tag{1}$$

$$\mathrm{PBIAS} = \frac{\sum_{i=1}^{n} 100\left(Q_i^{obs} - Q_i^{sim}\right)}{\sum_{i=1}^{n} Q_i^{obs}} \tag{2}$$

$$\mathrm{RSR} = \frac{\mathrm{RMSE}}{\mathrm{STDEV}_{obs}} = \frac{\sqrt{\sum_{i=1}^{n}\left(Q_i^{obs} - Q_i^{sim}\right)^2}}{\sqrt{\sum_{i=1}^{n}\left(Q_i^{obs} - Q_{mean}^{obs}\right)^2}} \tag{3}$$

where Q_i^{obs} and Q_i^{sim} are the observed and simulated values at time step i, Q_{mean}^{obs} the mean values of observations, and n the number of time steps.

2.4. Methodology for separating the impacts of climate change and LUCC on hydrology

The hydrological modelling with the one-factor-at-a-time (OFAT) analysis was employed to separate hydrological impacts of LUCC from those of climate change. The methodology consists of three steps, as mentioned in the section of Introduction. In the first step, the meteorological forcings of the entire study time span are typically split into two time-slices, of which the first ($C1$) is selected as the baseline period while the second ($C2$) as the comparative one. For both time periods, the land use conditions are represented by two land use maps ($L1$ and $L2$), respectively. As shown in Table 2, the OFAT modelling experiments (E1, E2, E3 and E4) are generally designed through the combinations of $C1$, $C2$, $L1$ and $L2$.

The absolute and relative contributions of LUCC and climate change to hydrological variations such as the changes in streamflow and ET are solved use the following equations:

$$\Delta Q_L = Q_{L2}^{C1} - Q_{L1}^{C1} \tag{4}$$

$$\Delta Q_C = Q_{L1}^{C2} - Q_{L1}^{C1} \tag{5}$$

$$\Delta Q = Q_{L2}^{C2} - Q_{L1}^{C1} \tag{6}$$

$$W_L = \frac{\Delta Q_L}{\Delta Q} \times 100\% \tag{7}$$

$$W_C = \frac{\Delta Q_C}{\Delta Q} \times 100\% \tag{8}$$

where ΔQ_L and ΔQ_C, ΔQ are the hydrological variations due to LUCC, climate change, and both LUCC and climate change, respectively; W_L and W_C are the relative contributions of LUCC and climate change, respectively; Q_{L1}^{C1}, Q_{L2}^{C1}, Q_{L1}^{C2} and Q_{L2}^{C2} are the mean annual values of the hydrological components simulated in the experiments of E1, E2, E3 and E4, respectively.

ΔQ is generally not equal to the sum of ΔQ_L and ΔQ_C, and, consequently, the overall relative contributions of LUCC and climate change (i.e., the sum of W_L and W_C) will not total to 100%. To avoid this problem, Yang et al. (2017) have recently proposed a new method, as in Eqs. (9), (10) and (11), to calculated the hydrological variations induced by LUCC, climate change and the joint LUCC and climate variability, respectively. This new approach was adopted in this study.

$$\Delta Q_L = \frac{1}{2}\left[\left(Q_{L2}^{C1} - Q_{L1}^{C1}\right) + \left(Q_{L2}^{C2} - Q_{L1}^{C2}\right)\right] \tag{9}$$

$$\Delta Q_C = \frac{1}{2}\left[\left(Q_{L1}^{C2} - Q_{L1}^{C1}\right) + \left(Q_{L2}^{C2} - Q_{L2}^{C1}\right)\right] \tag{10}$$

$$\Delta Q = \Delta Q_L + \Delta Q_C = Q_{L2}^{C2} - Q_{L1}^{C1} \tag{11}$$

2.5. Baseline period choices and hypothetical LUCC scenario

This study considered the hydrological impacts of LUCC and climate change over the recent 20 years (1995–2014). The individual contributions of LUCC and climate change to the variations in water yield and ET were isolated based on the meteorological forcings from 1995 to 2014 and the land use maps of 2000 and 2011. We assumed that two land use maps are able to represent the land use conditions for the baseline and comparative periods, respectively, when their observation time falls in corresponding periods. This assumption has implicitly been made in many other similar studies (e.g. Li et al., 2009a; Shi et al., 2013; Niraula et al., 2015; Alvarenga et al., 2016; Setyorini et al., 2017). Eleven baseline periods, i.e., 2000B, 2001B, 2002B, 2003B,

Table 2
OFAT modelling experiments designed to separate LUCC and climate change impacts on watershed hydrology.

Modelling experiment	Land use condition	Climatic condition
E1	$L1$	$C1$
E2	$L2$	$C1$
E3	$L1$	$C2$
E4	$L2$	$C2$

2004B, 2005B, 2006B, 2007B, 2008B, 2009B and 2010B, were thus determined from the entire time frame. The 2000B refers to the baseline period of 1995–2000; the 2001B refers to the baseline period of 1995–2001; and so on. These baseline periods were used to investigate the influences of baseline period choices on the partitioning of hydrological impacts. In this way, we can quantify how large the divergence of the influences of baseline period choices would be when using different hydrological models.

The absolute contributions of LUCC to the hydrological variations were estimated to be slight in the UHRB during the period 1995–2014 (Zhang et al., 2016). This is partly due to the insignificant changes in land use area in comparison with the size of the whole study area, and partly due to the compensating effects of LUCC on hydrology when assessing the basin-wide impacts. Thus, besides the real land use change between 2000 and 2011 (referred to as "real LUCC case"), an additional land-use change scenario (referred to as "hypothetical LUCC case") was developed. This scenario, which assumes grassland has completely converted to farmland in the year of 2011, is extreme and clearly hypothetical, but it serves the study purpose of evaluating the influences of baseline period choices on the separations of hydrological impacts in case that the changes in land use/cover are more obvious and substantial.

3. Results and discussion

3.1. Model calibration and validation

As reported in a previous study (Zhang et al., 2016), the SWAT model performs reasonably well in the study area, as indicated by a high value of NSE (>0.85), and low values of PBIAS (<11%) and RSR (<0.35) for monthly river discharge at the basin outlet. It proved to be applicable to the UHRB and can be used to separate the impacts of LUCC and climate variability on watershed hydrology.

Fig. 2 presents the comparisons of monthly and daily streamflow observations with the DHSVM simulations at the outlet of the UHRB. The model is able to well capture the dynamics of the hydrograph in both calibration and validation periods. Nevertheless, the simulation accuracy of peak flows is relatively low in most years, which is intimately related to the structure of the model. Peak flows are generally composed of three components including baseflow, preferential flow and overland flow (Du et al., 2014). The preferential flow, however, is not represented in the current version of the model, resulting in tradeoffs of the simulation precision between peak flows and baseflows (Beckers and Alila, 2004; Cuo et al., 2006). Meanwhile, the streamflow in March through June in each year tends to be underestimated by the model. This is partially due to the exponential decay assumption of DHSVM, i.e., the soil lateral saturated hydraulic conductivity decreases exponentially with soil depth. The water table is declining and would approach to the lowest level in winter, owing to the scarce precipitation and continuous groundwater discharge to streamflow. It begins to ascend with increasing precipitation during the months from March to June, causing rising lateral saturated hydraulic conductivity. However, according to the assumption, the increase rates at deeper watertable depths would be smaller than that at shallower depths, which may in turn underestimate baseflow and streamflow in the period of March through June. Moreover, the distinctive cryospheric processes in the UHRB such as soil freezing/thawing and glacier melting can also have a profound impact on the hydrological cycle. The absence of such processes in DHSVM may also be connect to the underestimation of streamflow.

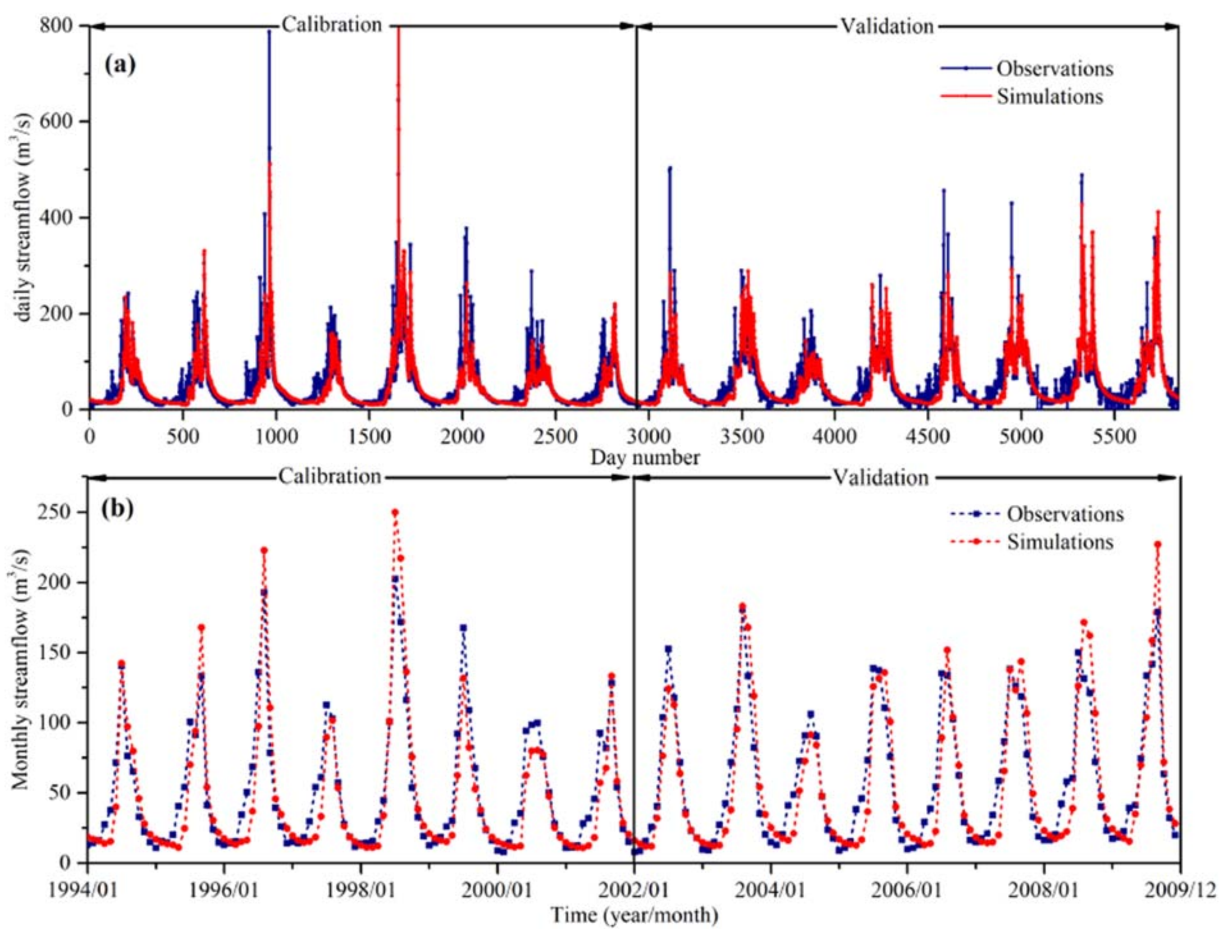

Fig. 2. Comparisons of the daily (a) and monthly (b) streamflow observations with the DHSVM simulations during calibration and validation periods.

Table 3
Efficiency metrics of DHSVM for daily and monthly streamflow simulations at the basin outlet during the calibration and validation periods.

Time step	Period	Efficiency metrics		
		NSE	PBIAS	RSR
Daily	Calibration (1994–2001)	0.741	6.53%	0.509
	Validation (2002–2009)	0.732	3.71%	0.517
Monthly	Calibration (1994–2001)	0.840	6.57%	0.400
	Validation (2002–2009)	0.822	3.72%	0.421

The efficiency statistics of DHSVM for daily and monthly streamflow simulations are summarized in Table 3. NSE, PBIAS and RSR are 0.741, 6.53% and 0.509, respectively, for the daily streamflow during the calibration period, and 0.732, 3.71% and 0.517, respectively, during the validation period. They are 0.840, 6.57% and 0.400, respectively, for the monthly streamflow during the calibration period, and 0.822, 3.72% and 0.421, respectively, during the validation period. According to the model evaluation guidelines proposed by Moriasi et al. (2007), we can conclude that the DHSVM model performs good in the UHRB and is able to serve the study purpose.

3.2. Contributions of LUCC and climate change to hydrological variations

3.2.1. Real LUCC case

In the real LUCC case, the absolute contributions of climate change and LUCC to the changes in water yield (i.e., the total amount of water intercepted by channels) and ET for different baseline period choices are presented in Fig. 3. Obviously, climate change contributed more significantly to the hydrological variations than LUCC regardless of baseline period choices. The LUCC induced changes in water yield and ET are slight, with almost the same magnitude for different baseline period selections. The climate change induced hydrological variations, however, are much obvious, with varying magnitudes for various baseline periods. The varying magnitudes of the changes in water yields and ET can be attributed to different changes in precipitation and temperature, the two most important factors leading to hydrological variation in the study area (Zhang et al., 2016). By comparing Figs. 3 and 4, it is seen that the baseline periods of 2000B, 2003B and 2009B generate relatively lower precipitation changes, in comparison to the other baseline periods, which in turn induce smaller variations in water yield. Moreover, the baseline periods of 2000B–2006B lead to relatively higher temperature changes, which in turn induce higher changes in ET (Sang et al., 2014), compared with the other baseline periods.

As shown in Fig. 3, the divergence of climate change-induced hydrological variations, particularly the changes in ET, due to various baseline period choices is different for the two models. For SWAT, the largest and smallest changes in water yield were resulted from the selection of the baseline periods of 2007B and 2000B, respectively, while for DHSVM, they were resulted from the 2006B and 2009B, respectively. Similar results can be observed from the changes in ET. This implies that the influence of baseline period choices on the partitioning of hydrological impacts can diverge significantly between different hydrological models. It is rather reasonable considering that the SWAT and DHSVM models vary in type, structure, spatial discretization and process representation, as outlined in Table 1. Taking the simulation of actual ET as an example, both the models mainly consist of three steps: (i) estimating potential ET, (ii) partitioning potential ET demands between soil layers; and (iii) determining the actual ET of each layer through balancing water demand and supply. However, the implementation of each step

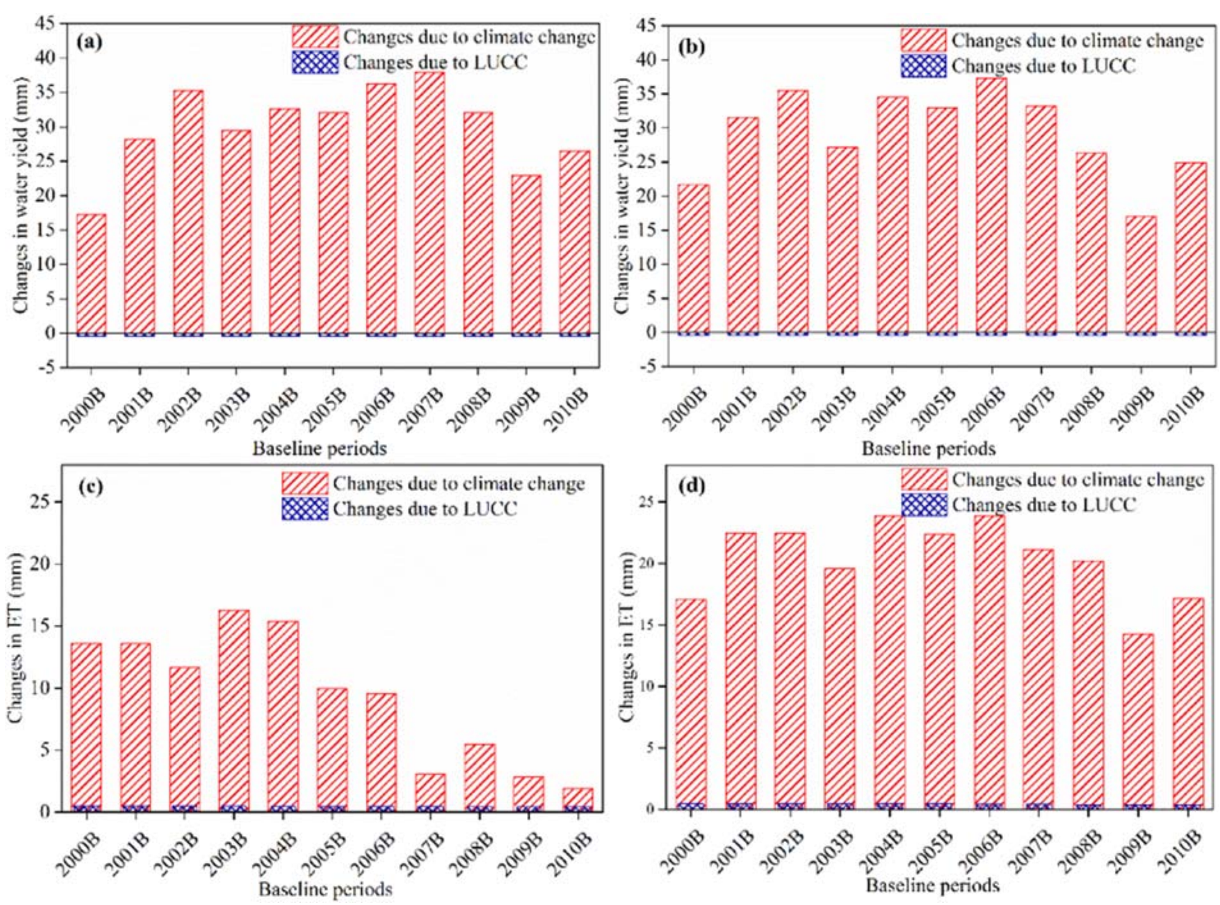

Fig. 3. Absolute contributions of climate change and LUCC to the changes in water yield (top) and ET (bottom) for different baseline period choices estimated by SWAT (left panel) and DHSVM (right panel) in the real LUCC case.

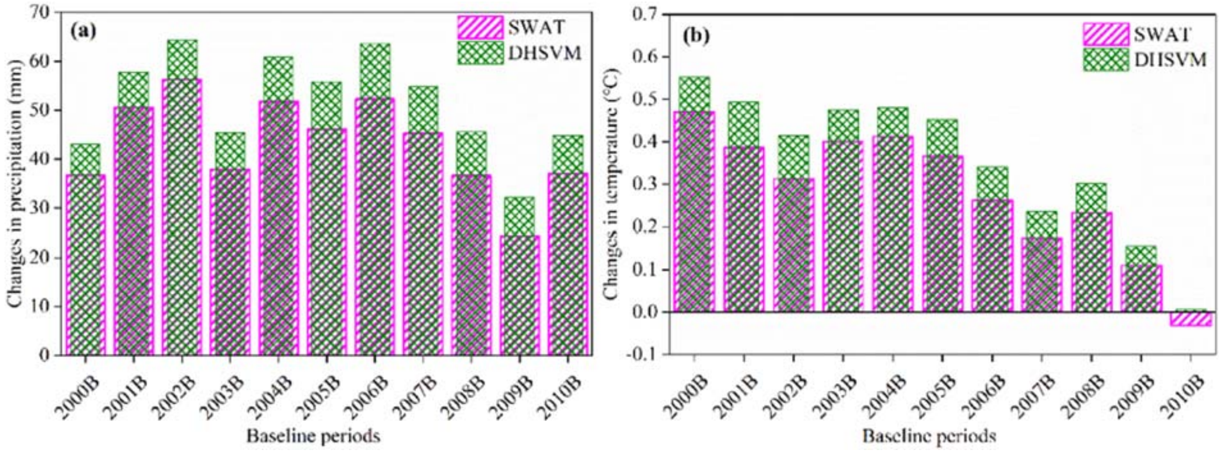

Fig. 4. Changes in precipitation (a) and temperature (b) over the UHRB for different baseline periods estimated using the SWAT and DHSVM models.

varies substantially between the models (Wigmosta et al., 1994; Neitsch et al., 2011). In the first step, SWAT only considers one layer of canopy in estimation of potential ET, whereas DHSVM does with two layers. Meanwhile, SWAT calculates canopy resistance based only on vapour pressure deficit whereas DHSVM based on air temperature, vapour pressure deficit and soil water content in the Penman-Monteith approach (Breuer et al., 2009). In the second step, SWAT partitions the potential ET demand based on an empirical attenuation curve whereas DHSVM is based on the root proportion of each soil layer. In the final step, SWAT limits the minimum and maximum water that can be removed from each soil layer whereas DHSVM not. Moreover, the varying influences of baseline period choices can also be explained by that the two models adopt different interpolation method to obtain the spatial patterns of climate variables over the study domain. The SWAT uses the nearest neighbourhood approach that only considers the influence of distance, whereas DHSVM applies the Cressman interpolation scheme that takes both the effects of distance and elevation into account. As a result, the divergence of the changes of climate variables such as precipitation and temperature, resulting from choosing different baseline periods, vary between the models, as presented in Fig. 4.

Figs. 5 and 6 show the absolute contributions of climate change and LUCC to hydrological variations on a monthly scale when choosing different baseline periods. Either climate change or LUCC contributes to obvious water yield changes in the wet months from May to September. By looking at different baseline period choices, it is seen that the magnitudes of the changes in water yield due to climate change differ pronouncedly during the wet months. The changes in water yield even show reverse trends in some months for the baseline periods of 2009B and 2010B, in comparison with the other baseline periods. The magnitude of the changes in water yield due to LUCC, however, shows little

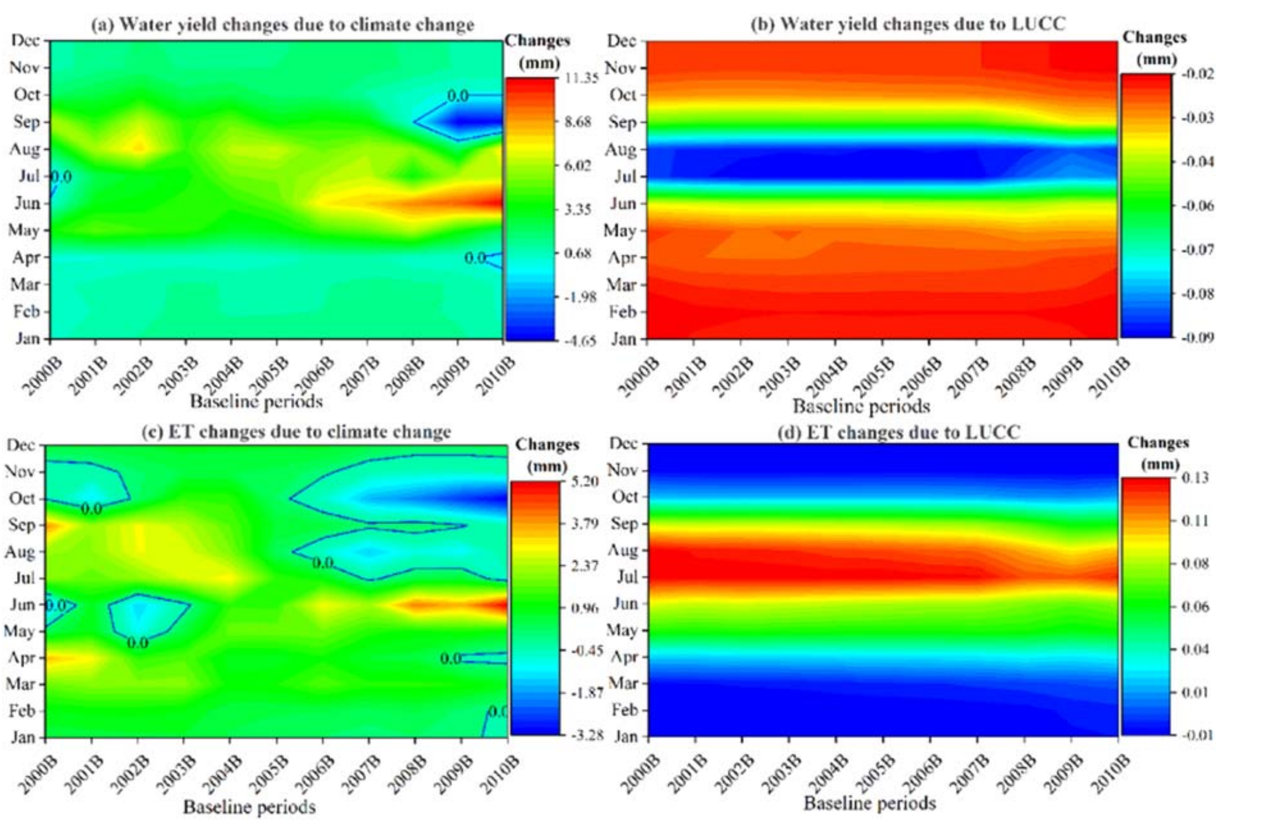

Fig. 5. Absolute contributions of climate change (left) and LUCC (right) to the changes in monthly water yield (top) and ET (bottom) estimated using SWAT with different baseline periods.

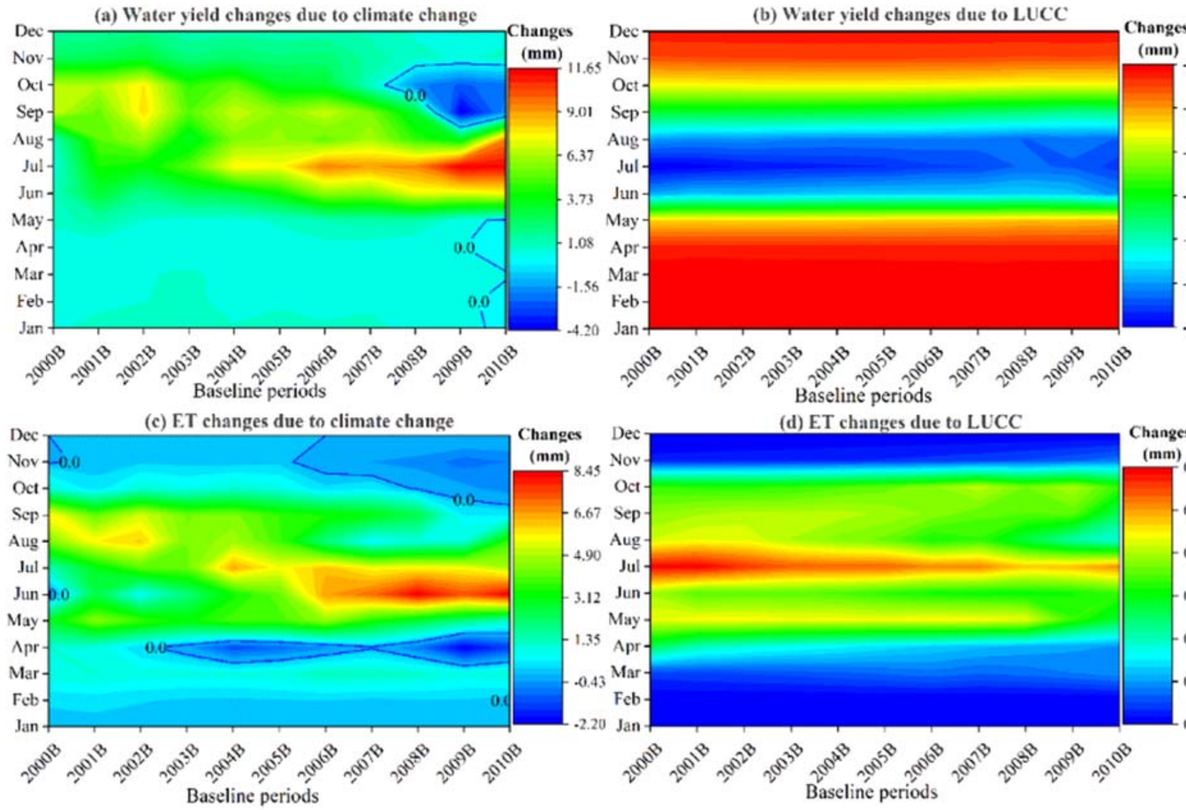

Fig. 6. Absolute contributions of climate change (left) and LUCC (right) to the changes in monthly water yield (top) and ET (bottom) estimated using DHSVM with different baseline periods.

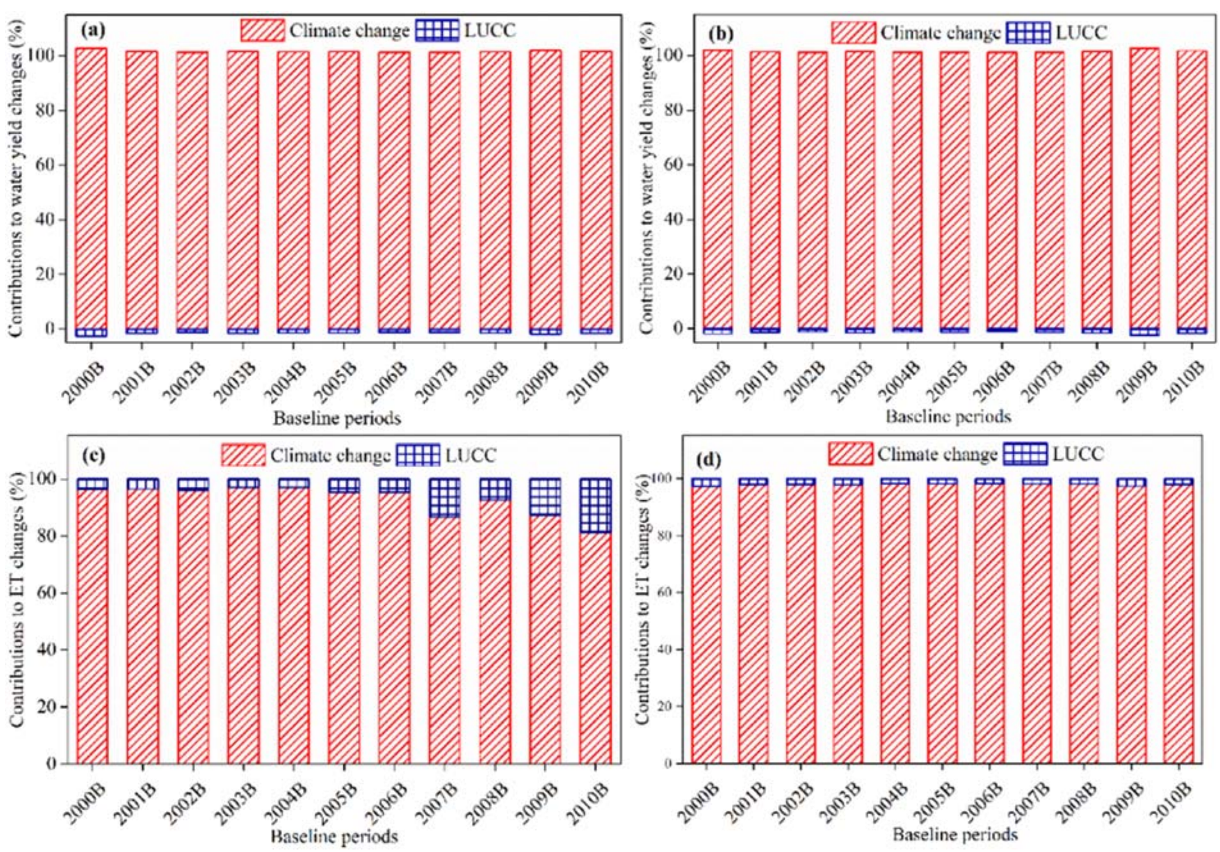

Fig. 7. Relative contributions of climate change and LUCC to the changes in water yield (top) and ET (bottom) for different baseline period choices estimated by SWAT (left) and DHSVM (right panel) in the real LUCC case.

divergence between different baseline periods. Very similar results can be observed in the changes in ET. Comparing the results of two models, we concluded that the varying influence of baseline period choices on the partitioning of impacts is more obvious on the ET changes than on the water yield changes.

Fig. 7 depicts the relative contributions of climate change and LUCC to hydrological variations. As for the changes in water yield, the relative contributions diverge insignificantly between different baseline period choices, owing to the more obviously absolute contribution of climate change than that of LUCC. The relative contributions of climate change and LUCC are modeled to be 101–102% and −2–−1%, respectively for various baseline periods. As for the changes in ET, a higher relative contribution of climate change (>95%) than that of LUCC (<5%) is simulated for the baseline periods from 2000B to 2006B. However, for the other baseline periods (i.e., 2007B–2010B), the relative contributions of LUCC are estimated to be <5% by DHSVM while >5% by SWAT.

3.2.2. Hypothetical LUCC case

In the hypothetical LUCC case, the absolute hydrological contributions of climate change and LUCC for different baseline period choices are presented in Fig. 8. It is clear that both climate change and LUCC contribute significantly to the changes in water yield and ET. Similar to the real LUCC case, the magnitudes of the hydrological variations due to climate change vary significantly between various baseline period selections. The changes in water yield and ET due to LUCC present apparent decreasing and increasing trends, respectively, for SWAT over the baseline periods from 2000B to 2010B, although they show very slight trends for DHSVM.

Fig. 9 illustrates the relative contributions of climate change and LUCC to the changes in water yield and ET. Apparently, the magnitudes and directions of the relative contributions to the changes in water yield vary in different baseline periods. Positive contributions of LUCC and negative contributions of climate change are simulated by SWAT for the baseline periods of 2000B, 2009B and 2010B, while reverse contributions for the other baseline period selections. For DHSVM, the 2009B is the only baseline period that results in positive contribution of LUCC and negative contribution of climate change to the changes in water yield. The other baseline period choices led to opposite results. The relative contributions of LUCC and climate change estimated by the SWAT and DHSVM models are opposite for the baseline periods of 2000B and 2010B. The two models estimate varying magnitudes of hydrological variations due to LUCC or climate change. It is seen in Fig. 8 that the absolute contribution of LUCC estimated by SWAT is greater than that of climate change for the baseline periods of 2000B and 2010B. However, the opposite is observed for DHSVM. Consequently, the combined effects of climate change and LUCC are modeled to be negative and positive by SWAT and DHSVM, respectively. It signifies opposite roles of LUCC and climate change in terms of relative contributions. The relative contributions of LUCC and climate change to the changes in ET show upward and downward trends, respectively, over the baseline period choices from 2000B to 2010B, according to the SWAT simulation. Nevertheless, they exhibit no clear trends and fall within 40–60% when DHSVM was used.

3.3. Uncertainty reduction associated with baseline period choices

The results demonstrated that the isolated impacts can diverge significantly between different baseline period choices. Thus, the baseline period choice is an important source of uncertainties when disentangling the impacts of climate change and LUCC using the hydrological

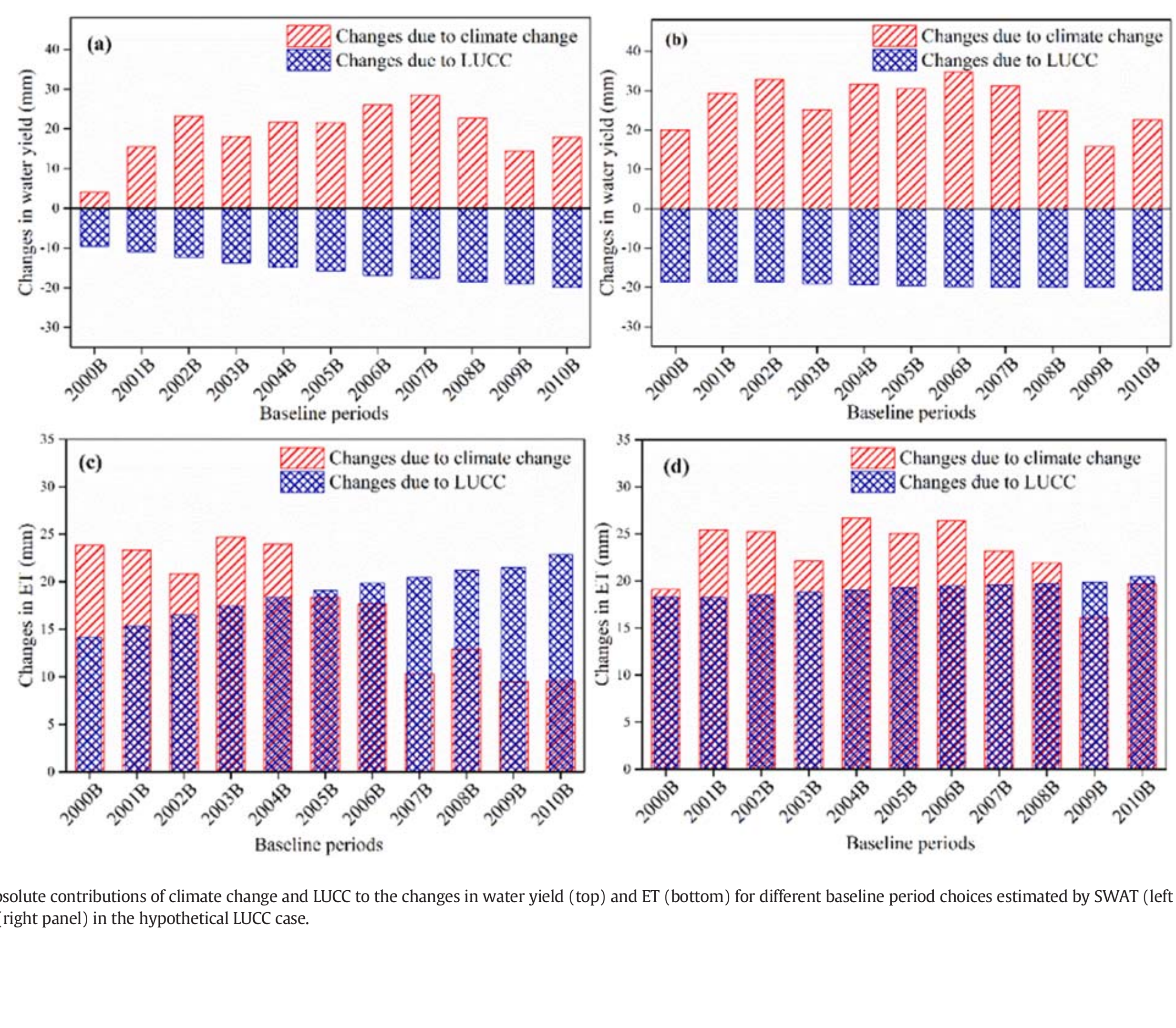

Fig. 8. Absolute contributions of climate change and LUCC to the changes in water yield (top) and ET (bottom) for different baseline period choices estimated by SWAT (left panel) and DHSVM (right panel) in the hypothetical LUCC case.

modelling and OFAT approach. Since the distinguished hydrological impacts heavily depend on the selected baselined periods, we argue that it is important to consider and discuss the condition of which baseline period was adopted at the time concluding the individual and relative contributions of climate change and LUCC to hydrological variations. It should be cautious when two studies with different baseline periods being adopted are compared for evaluating isolated impacts of LUCC and climate changes. In other words, the comparisons can be made upon consistency of baseline periods.

However, it is hard to figure out a general rule of thumb applicable to the selection of the most proper baseline period. Nevertheless, some useful recommendations can be offered, which may help to reduce the uncertainties associated with baseline period choices.

First, the length of the baseline period can't be too short or too long. As shown in the real and hypothetical cases, the baseline period of 2000B, which has the smallest length (i.e., 6 years), tends to cause improper contributions of climate change and LUCC, compared with the baseline periods from 2001B to 2008B. Meanwhile, the length of the baseline period could not be too long if the entire study period has been determined, as it will lead the comparative period to be very short. The baseline periods of 2009B and 2010B, which have larger lengths (i.e., 15 and 16 years), are likely to result in different separation of hydrological impacts, compared with the baseline periods from 2001B to 2008B. Too short baseline period or comparative period is insufficient in representing an average climatic condition and is likely to over- or under-estimate the isolated hydrological impacts.

Second, reliable land use maps representing the land use/cover conditions in the baseline period are necessary for reducing uncertainty. The most common approach is to ensure the observation time of a land use map falls within the baseline period. However, if the land use/cover have changed substantially over the baseline period or baseline period is relatively long, one land use map may not be able to fully represent the land use/cover conditions, and as a result, the contribution of LUCC to hydrological variations may be underestimated. In these cases, it is necessary to include two or more land use maps, if possible, to fully characterize the dynamics of land use/cover conditions over the baseline period (Wagner et al., 2017).

Third, the baseline period should be selected by considering the goal of the research. For example, if there is a land-use policy that has been implemented in the study area within the study period and we want to figure out its impacts on the hydrological variations as well as its relative contribution in comparison to that of climate change, it will be more appropriate to select the year for implementing the policy as the dividing point to determine the baseline period. For another instance, if the research focus on the influences of LUCC and climate change between two different ages such as 1980s and 1990s, then it will be more appropriate to directly choose the former age as the baseline period, as in the study of Luo et al. (2016).

Last but not least, some pre-analyses are usually helpful in choosing an appropriate baseline period. For example, one can detect the temporal trends and change points of the observed hydrological variables such as runoff using the non-parametric method, and then select the first period before the change point as the baseline period. A similar method can be found in Zuo et al. (2016). In most cases, the baseline period is determined as a part of the entire study time span. Actually, when climate varies over a long-time period, the beginning and ending conditions could represent the beginning and ending status of the changes (Cuo et al., 2013). Thus, one can first generate the beginning and the ending climate records by subtracting and adding climate change trends from (to) the meteorological forcing over the entire study time frame; and then choose them as the baseline and comparative periods, respectively.

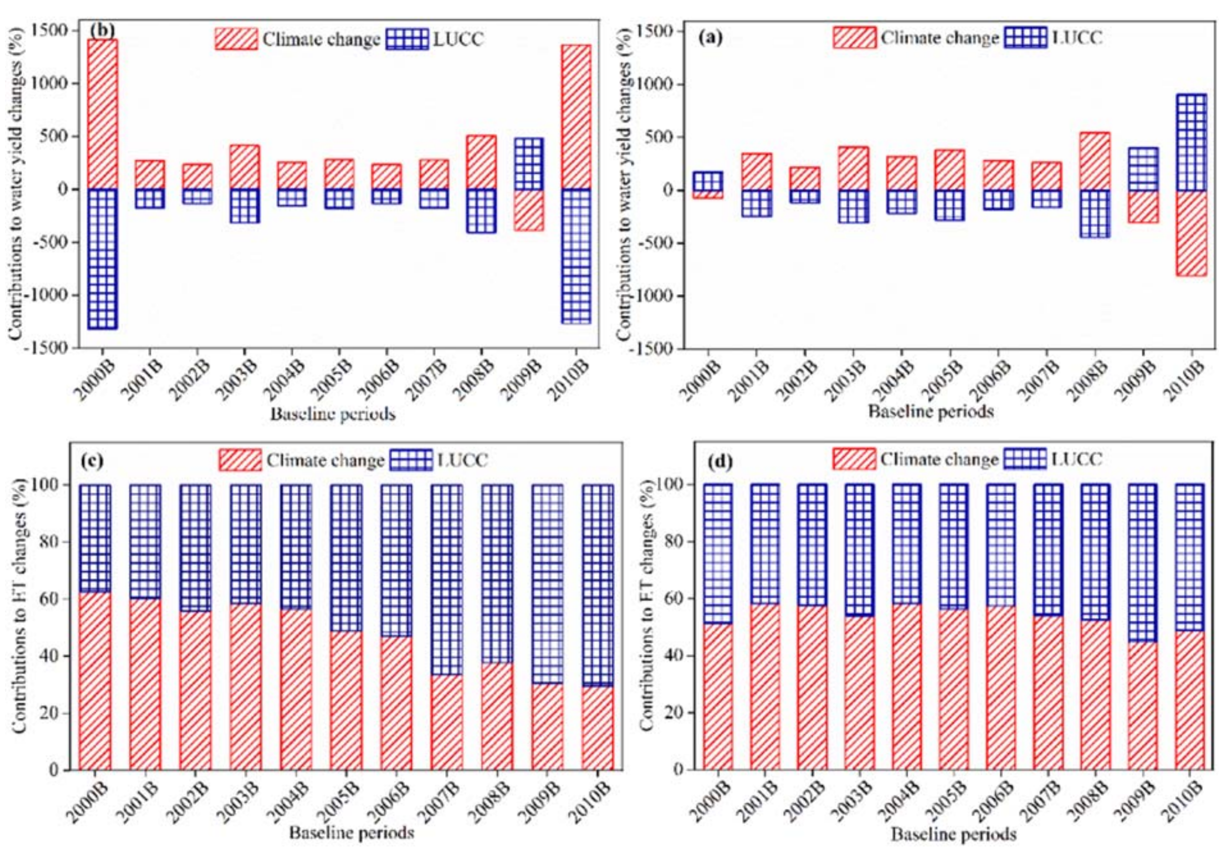

Fig. 9. Relative contributions of climate change and LUCC to the changes in water yield (top) and ET (bottom) for different baseline period choices estimated by SWAT (left panel) and DHSVM (right panel) in the hypothetical LUCC case.

4. Conclusions

This study was mainly conducted to compare baseline period choices for separating impacts of climate change and LUCC on watershed hydrology. Towards this purpose, we applied the SWAT and DHSVM models with various baseline periods to a typical inland river basin in northwest China.

In the real LUCC case that considers the actual land use changes between 2000 and 2011, the absolute contributions of LUCC to the changes in water yield and ET are slight and almost have the same magnitude for various baseline period choices, while those of climate change are substantial and have obviously different magnitudes. On a monthly time scale, with various baseline period selections, the two models simulated similar patterns of changes in water yield due to LUCC or climate change, but apparently different patterns of variations in ET. Meanwhile, the divergence of hydrological variations between different baseline period selections mainly lies in the wet months from May to September. As for the relative contributions of LUCC or climate change, they diverge insignificantly between different baseline period choices, and seem less sensitive to the choices of baseline periods, compared with the absolute contributions. In the hypothetical LUCC case which assumes an extreme land use conversion (i.e., grassland converts to farmland completely), both climate change and LUCC contribute to the changes in water yield and ET significantly. Moreover, both the absolute and relative contributions diverge noticeably between various baseline period choices. The influence of baseline period choices on the partitioning of hydrological impacts diverge significantly between different hydrological models.

This study highlights the separated impacts of climate change and LUCC on hydrology would be significantly different depending on the selected baseline periods. Thus, the choice of baseline period is an important source of uncertainties when disentangling the impacts of climate change and LUCC using the hydrological modelling and OFAT approach. It is difficult to give a standard method for choosing baseline periods in this study. Nevertheless, some useful recommendations proposed in this study are likely to be helpful to reduce the uncertainties associated with baseline period choices.

Acknowledgements

This work was supported in part by the National Science Foundation of China (NSFC) (grant numbers 91425303, 41671373 and 91625103) and in part by Natural Science Program Jiangsu Higher Education Institutions (17KJA170003). The authors thank the China Meteorological Data Sharing Service System (http://cdc.nmic.cn/) and the Science Data Center for Cold and Arid Regions (http://westdc.westgis.ac.cn) for data provision. The authors also greatly appreciate the constructive comments and recommendations of the three anonymous reviewers.

References

Alvarenga, L.A., de Mello, C.R., Colombo, A., Cuartas, L.A., Bowling, L.C., 2016. Assessment of land cover change on the hydrology of a Brazilian headwater watershed using the distributed hydrology-soil-vegetation model. Catena 143, 7–17.

Arnold, J.G., Srinivasan, R., Muttiah, R.S., Williams, J.R., 1998. Large area hydrologic modelling and assessment. Part I: model development. J. Am. Water Resour. Assoc. 34 (1), 73–89.

Baker, T.J., Miller, S.N., 2013. Using the soil and water assessment tool (SWAT) to assess land use impact on water resources in an east African watershed. J. Hydrol. 486, 100–111.

Beckers, J., Alila, Y., 2004. A model of rapid preferential hillslope runoff contributions to peak flow generation in a temperate rain forest watershed. Water Resour. Res. 40 (3). https://doi.org/10.1029/2003WR002582.

Bieger, K., Hörmann, G., Fohrer, N., 2015. The impact of land use change in the Xiangxi catchment (China) on water balance and sediment transport. Reg. Environ. Chang. 15 (3), 485–498.

Bosch, J.M., Hewlett, J.D., 1982. A review of catchment experiments to determine the effect of vegetation changes on water yield and evapotranspiration. J. Hydrol. 55 (1–4), 3–23.

Breuer, L., et al., 2009. Assessing the impact of land use change on hydrology by ensemble modeling (LUCHEM). I: model intercomparison with current land use. Adv. Water Resour. 32 (2), 129–146.

Brown, A.E., Zhang, L., McMahon, T.A., Western, A.W., Vertessy, R.A., 2005. A review of paired catchment studies for determining changes in water yield resulting from alterations in vegetation. J. Hydrol. 310 (1–4), 28–61.

Chen, H., Xu, C.-Y., Guo, S., 2012. Comparison and evaluation of multiple GCMs, statistical downscaling and hydrological models in the study of climate change impacts on runoff. J. Hydrol. 434, 36–45.

Choi, W., 2008. Catchment-scale hydrological response to climate-land-use combined scenarios: a case study for the Kishwaukee River basin, Illinois. Phys. Geogr. 29 (1): 79–99. https://doi.org/10.2747/0272-3646.29.1.79.

Cong, Z., Shahid, M., Zhang, D., Lei, H., Yang, D., 2017. Attribution of runoff change in the alpine basin: a case study of the Heihe Upstream Basin, China. Hydrol. Sci. J. 62 (6), 1013–1028.

Cornelissen, T., Diekkrüger, B., Giertz, S., 2013. A comparison of hydrological models for assessing the impact of land use and climate change on discharge in a tropical catchment. J. Hydrol. 498, 221–236.

Cuartas, L.A., et al., 2012. Distributed hydrological modeling of a micro-scale rainforest watershed in Amazonia: model evaluation and advances in calibration using the new HAND terrain model. J. Hydrol. 462–463, 15–27.

Cuo, L., 2016. Land use/cover change impacts on hydrology in large river basins. In: Tang, Q., Oki, T. (Eds.), Terrestrial Water Cycle and Climate Change: Natural and Human-Induced Impacts. John Wiley & Sons, Inc (103–134 pp).

Cuo, L., Giambelluca, T.W., Ziegler, A.D., Nullet, M.A., 2006. Use of the distributed hydrology soil vegetation model to study road effects on hydrological processes in Pang Khum experimental watershed, northern Thailand. For. Ecol. Manag. 224 (1–2), 81–94.

Cuo, L., Lettenmaier, D.P., Alberti, M., Richey, J.E., 2009. Effects of a century of land cover and climate change on the hydrology of the Puget Sound basin. Hydrol. Process. 23 (6), 907–933.

Cuo, L., Zhang, Y., Gao, Y., Hao, Z., Cairang, L., 2013. The impacts of climate change and land cover/use transition on the hydrology in the upper Yellow River basin, China. J. Hydrol. 502, 37–52.

Dang, S., Liu, C., Wang, Z., Wu, M., 2012. Spatio-temporal distribution characteristics of snow cover in the upper reaches of Heihe River basin over the past 10 years and the variation trend (in Chinese). Resour. Sci. 34 (8), 1574–1581.

Dey, P., Mishra, A., 2017. Separating the impacts of climate change and human activities on streamflow: a review of methodologies and critical assumptions. J. Hydrol. 548, 278–290.

Dickerson-Lange, S.E., Mitchell, R., 2014. Modeling the effects of climate change projections on streamflow in the Nooksack River basin, Northwest Washington. Hydrol. Process. 28 (20), 5236–5250.

Du, E., Link, T.E., Gravelle, J.A., Hubbart, J.A., 2014. Validation and sensitivity test of the distributed hydrology soil-vegetation model (DHSVM) in a forested mountain watershed. Hydrol. Process. 28 (26), 6196–6210.

Franczyk, J., Chang, H., 2009. The effects of climate change and urbanization on the runoff of the Rock Creek basin in the Portland metropolitan area, Oregon, USA. Hydrol. Process. 23 (6), 805–815.

Gao, G., Fu, B., Wang, S., Liang, W., Jiang, X., 2016. Determining the hydrological responses to climate variability and land use/cover change in the Loess Plateau with the Budyko framework. Sci. Total Environ. 557, 331–342.

Guo, J., Su, X., Singh, V., Jin, J., 2016. Impacts of climate and land use/cover change on streamflow using SWAT and a separation method for the Xiying River basin in northwestern China. Water 8 (5):192. https://doi.org/10.3390/w8050192.

Hao, X., Wang, J., Che, T., Zhang, P., Liang, J., Li, H., Li, Z., Bai, Y., Bai, Y., 2009. The spatial distribution and properties of snow cover in Binggou watershed, Qilian Mountains: measurement and analysis (in Chinese). J. Glaciol. Geocryol. 31 (2), 284–292.

Hu, X., Lu, L., Li, X., Wang, J., Guo, M., 2015. Land use/cover change in the middle reaches of the Heihe River basin over 2000–2011 and its implications for sustainable water resource management. PLoS One 10 (6), e0128960.

Jiang, T., Chen, Y.D., Xu, C.-Y., Chen, X., Chen, X., Singh, V.P., 2007. Comparison of hydrological impacts of climate change simulated by six hydrological models in the Dongjiang Basin, South China. J. Hydrol. 336 (3), 316–333.

Karlsson, I.B., Sonnenborg, T.O., Refsgaard, J.C., Trolle, D., Børgesen, C.D., Olesen, J.E., Jeppesen, E., Jensen, K.H., 2016. Combined effects of climate models, hydrological model structures and land use scenarios on hydrological impacts of climate change. J. Hydrol. 535, 301–317.

Khoi, D.N., Suetsugi, T., 2014. The responses of hydrological processes and sediment yield to land-use and climate change in the Be River Catchment, Vietnam. Hydrol. Process. 28 (3), 640–652.

Kim, J., Choi, J., Choi, C., Park, S., 2013. Impacts of changes in climate and land use/land cover under IPCC RCP scenarios on streamflow in the Hoeya River basin, Korea. Sci. Total Environ. 452, 181–195.

Kundu, S., Khare, D., Mondal, A., 2017. Individual and combined impacts of future climate and land use changes on the water balance. Ecol. Eng. 105, 42–57.

Lai, Z., Li, S., Li, C., Nan, Z., Yu, W., 2013. Improvement and applications of SWAT model in the upper-middle Heihe River basin (in Chinese). J. Nat. Resour. 28 (8), 1404–1413.

Li, C., 2012. Study on Improvement of SWAT Model and Integrated Simulation in the Upper-middle Heihe River Basin (in Chinese). Nanjing Normal University.

Li, Z., Liu, W.-z., Zhang, X.-c., Zheng, F.-l, 2009. Impacts of land use change and climate variability on hydrology in an agricultural catchment on the Loess Plateau of China. J. Hydrol. 377 (1), 35–42.

Li, Z., Xu, Z., Shao, Q., Yang, J., 2009. Parameter estimation and uncertainty analysis of SWAT model in upper reaches of the Heihe river basin. Hydrol. Process. 23 (19): 2744–2753. https://doi.org/10.1002/hyp.7371.

Li, H., Zhang, Y., Vaze, J., Wang, B., 2012. Separating effects of vegetation change and climate variability using hydrological modelling and sensitivity-based approaches. J. Hydrol. 420:403–418. https://doi.org/10.1016/j.jhydrol.2011.12.033.

Liang, X., Lettenmaier, D.P., Wood, E.F., Burges, S.J., 1994. A simple hydrologically based model of land surface water and energy fluxes for general circulation models. J. Geophys. Res. Atmos. 99 (D7), 14415–14428.

Liston, G.E., Elder, K., 2006. A meteorological distribution system for high-resolution terrestrial modeling (MicroMet). J. Hydrometeorol. 7 (2):217–234. https://doi.org/10.1175/JHM486.1.

Livneh, B., Rosenberg, E.A., Lin, C., Nijssen, B., Mishra, V., Andreadis, K.M., Maurer, E.P., Lettenmaier, D.P., 2013. A long-term hydrologically based dataset of land surface fluxes and states for the conterminous United States: update and extensions. J. Clim. 26 (23), 9384–9392.

Lu, L., Liu, C., Li, X., 2011. Soil Texture Dataset of the Heihe River Basin (2011). Heihe Plan Science Data Center https://doi.org/10.3972/heihe.023.2013.db.

Luo, K., Tao, F., Moiwo, J.P., Xiao, D., 2016. Attribution of hydrological change in Heihe River basin to climate and land use change in the past three decades. Sci. Rep. 6.

McCormick, B.C., Eshleman, K.N., Griffith, J.L., Townsend, P.A., 2009. Detection of flooding responses at the river basin scale enhanced by land use change. Water Resour. Res. 45 (8) (n/a-n/a). https://doi.org/10.1029/2008WR007594.

Molina-Navarro, E., Trolle, D., Martínez-Pérez, S., Sastre-Merlín, A., Jeppesen, E., 2014. Hydrological and water quality impact assessment of a Mediterranean limno-reservoir under climate change and land use management scenarios. J. Hydrol. 509, 354–366.

Morán Tejeda, E., Zabalza, J., Rahman, K., Gago Silva, A., López Moreno, J.I., Vicente Serrano, S., Lehmann, A., Tague, C.L., Beniston, M., 2015. Hydrological impacts of climate and land-use changes in a mountain watershed: uncertainty estimation based on model comparison. Ecohydrology 8 (8), 1396–1416.

Moriasi, D., Arnold, J., Van Liew, M., Bingner, R., Harmel, R., Veith, T., 2007. Model evaluation guidelines for systematic quantification of accuracy in watershed simulations. Trans. ASABE 50 (3), 885–900.

Nash, J., Sutcliffe, J.V., 1970. River flow forecasting through conceptual models part I—a discussion of principles. J. Hydrol. 10 (3):282–290. https://doi.org/10.1016/0022-1694(70)90255-6.

Natkhin, M., Dietrich, O., Schäfer, M.P., Lischeid, G., 2015. The effects of climate and changing land use on the discharge regime of a small catchment in Tanzania. Reg. Environ. Chang. 15 (7), 1269–1280.

Neitsch, S.L., Arnold, J.G., Kiniry, J.R., Williams, J.R., 2011. Soil and Water Assessment Tool Theoretical Documentation: Version 2009. Texas Water Resources Institute (1–24 pp).

Niraula, R., Meixner, T., Norman, L.M., 2015. Determining the importance of model calibration for forecasting absolute/relative changes in streamflow from LULC and climate changes. J. Hydrol. 522, 439–451.

Pechlivanidis, I.G., Arheimer, B., Donnelly, C., Hundecha, Y., Huang, S., Aich, V., Samaniego, L., Eisner, S., Shi, P., 2016. Analysis of hydrological extremes at different hydro-climatic regimes under present and future conditions. Clim. Chang. 1–15.

Qi, S., Sun, G., Wang, Y., McNulty, S.G., Myers, J.A.M., 2009. Streamflow response to climate and landuse changes in a coastal watershed in North Carolina. Trans. ASABE 52 (3), 739–749.

Sang, Y.-F., Wang, Z., Liu, C., Yu, J., 2014. The impact of changing environments on the runoff regimes of the arid Heihe River basin, China. Theor. Appl. Climatol. 115 (1–2): 187–195. https://doi.org/10.1007/s00704-013-0888-y.

Setyorini, A., Khare, D., Pingale, S.M., 2017. Simulating the impact of land use/land cover change and climate variability on watershed hydrology in the upper Brantas basin, Indonesia. Appl. Geomatics https://doi.org/10.1007/s12518-017-0193-z.

Shi, P., Ma, X., Hou, Y., Li, Q., Zhang, Z., Qu, S., Chen, C., Cai, T., Fang, X., 2013. Effects of land-use and climate change on hydrological processes in the upstream of Huai River, China. Water Resour. Manag. 27 (5), 1263–1278.

Sorribas, M.V., Paiva, R.C.D., Melack, J.M., Bravo, J.M., Jones, C., Carvalho, L., Beighley, E., Forsberg, B., Costa, M.H., 2016. Projections of climate change effects on discharge and inundation in the Amazon basin. Clim. Chang. 136 (3–4), 555–570.

Storck, P., Bowling, L., Wetherbee, P., Lettenmaier, D., 1998. Application of a GIS-based distributed hydrology model for prediction of forest harvest effects on peak stream flow in the Pacific northwest. Hydrol. Process. 12 (6), 889–904.

Sunde, M.G., He, H.S., Hubbart, J.A., Urban, M.A., 2017. Integrating downscaled CMIP5 data with a physically-based hydrologic model to estimate potential climate change impacts on streamflow processes in a mixed-use watershed. Hydrol. Process. 31 (9), 1790–1803.

Thanapakpawin, P., Richey, J., Thomas, D., Rodda, S., Campbell, B., Logsdon, M., 2007. Effects of landuse change on the hydrologic regime of the Mae Chaem river basin, NW Thailand. J. Hydrol. 334 (1–2), 215–230.

Tian, Y., et al., 2015. Exploring scale-dependent ecohydrological responses in a large endorheic river basin through integrated surface water-groundwater modeling. Water Resour. Res. 51 (6), 4065–4085.

Tomer, M.D., Schilling, K.E., 2009. A simple approach to distinguish land-use and climate-change effects on watershed hydrology. J. Hydrol. 376 (1):24–33. https://doi.org/10.1016/j.jhydrol.2009.07.029.

Trang, N.T.T., Shrestha, S., Shrestha, M., Datta, A., Kawasaki, A., 2017. Evaluating the impacts of climate and land-use change on the hydrology and nutrient yield in a transboundary river basin: a case study in the 3S river basin (Sekong, Sesan, and Srepok). Sci. Total Environ. 576, 586–598.

Tu, J., 2009. Combined impact of climate and land use changes on streamflow and water quality in eastern Massachusetts, USA. J. Hydrol. 379 (3), 268–283.

Voisin, N., Liu, L., Hejazi, M., Tesfa, T., Li, H., Huang, M., Liu, Y., Leung, L.R., 2013. One-way coupling of an integrated assessment model and a water resources model: evaluation and implications of future changes over the US Midwest. Hydrol. Earth Syst. Sci. 17 (11), 4555–4575.

Wagner, P.D., Bhallamudi, S.M., Narasimhan, B., Kumar, S., Fohrer, N., Fiener, P., 2017. Comparing the effects of dynamic versus static representations of land use change in hydrologic impact assessments. Environ. Model. Softw. https://doi.org/10.1016/j.envsoft.2017.06.023.

Wang, J., Ge, C., Zhao, J., Hu, X., 2014. Landuse/Landcover Data of the Heihe River Basin in 2011. Heihe Plan Science Data Center https://doi.org/10.3972/heihe.093.2014.db.

Wang, Y., Yang, D., Lei, H., Yang, H., 2015. Impact of cryosphere hydrological processes on the river runoff in the upper reaches of Heihe River (in Chinese). J. Hydraul. Eng. 46 (9), 1064–1071.

Wang, S., Zhang, Z., McVicar, R.T., Guo, J., Tang, Y., Yao, A., 2013. Isolating the impacts of climate change and land use change on decadal streamflow variation: assessing three complementary approaches. J. Hydrol. 507, 63–74.

Wang, J., Zhao, J., Hu, X., Ge, C., 2014. Landuse/Landcover Data of the Heihe River Basin in 2000. Heihe Plan Science Data Center. https://doi.org/10.3972/heihe.039.2014.db.

Wei, X., Zhang, M., 2010. Quantifying streamflow change caused by forest disturbance at a large spatial scale: a single watershed study. Water Resour. Res. 46 (12) (n/a-n/a). https://doi.org/10.1029/2010WR009250.

Wigmosta, M.S., Perkins, W.A., 2001. Simulating the Effects of Forest Roads on Watershed Hydrology, Land Use and Watersheds: Human Influence on Hydrology and Geomorphology in Urban and Forest Areas. American Geophysical Union.

Wigmosta, M.S., Vail, L.W., Lettenmaier, D.P., 1994. A distributed hydrology-vegetation model for complex terrain. Water Resour. Res. 30 (6), 1665–1679.

Wu, F., Zhan, J., Chen, J., He, C., Zhang, Q., 2015. Water yield variation due to forestry change in the head-water area of Heihe River Basin, Northwest China. Adv. Meteorol., 786764 https://doi.org/10.1155/2015/786764.

Wu, F., Zhan, J., Su, H., Yan, H., Ma, E., 2014. Scenario-based impact assessment of land use/cover and climate changes on watershed hydrology in Heihe River Basin of northwest China. Adv. Meteorol. https://doi.org/10.1155/2015/410198.

Yan, R., Gao, J., Li, L., 2016. Modeling the hydrological effects of climate and land use/cover changes in Chinese lowland polder using an improved WALRUS model. Hydrol. Res. 47 (S1), 84.

Yang, L., Feng, Q., Yin, Z., Wen, X., Si, J., Li, C., Deo, R.C., 2017. Identifying separate impacts of climate and land use/cover change on hydrological processes in upper stream of Heihe River, Northwest China. Hydrol. Process. 31 (5), 1100–1112.

Yin, J., He, F., Xiong, Y.J., Qiu, G.Y., 2017. Effects of land use/land cover and climate changes on surface runoff in a semi-humid and semi-arid transition zone in northwest China. Hydrol. Earth Syst. Sci. 21 (1), 183–196.

Yu, W., Zhao, Y., Nan, Z., Li, S., 2013. Improvement of snowmelt implementation in the SWAT hydrologic model (in Chinese). Acta Ecol. Sin. 33 (21). https://doi.org/10.5846/stxb201207110977.

Zhang, L., Karthikeyan, R., Bai, Z., Srinivasan, R., 2017. Analysis of streamflow responses to climate variability and land use change in the Loess Plateau region of China. Catena 154, 1–11.

Zhang, A., Liu, W., Yin, Z., Fu, G., Zheng, C., 2016. How will climate change affect the water availability in the Heihe River basin, Northwest China? J. Hydrometeorol. 17 (5), 1517–1542.

Zhang, L., Nan, Z., Xu, Y., Li, S., 2016. Hydrological impacts of land use change and climate variability in the headwater region of the Heihe River basin, Northwest China. PLoS One 11 (6), e0158394. https://doi.org/10.1371/journal.pone.0158394.

Zhang, L., Nan, Z., Yu, W., Ge, Y., 2015. Modeling land-use and land-cover change and hydrological responses under consistent climate change scenarios in the Heihe River basin, China. Water Resour. Manag. 29 (13), 4701–4717.

Zhang, L., Nan, Z., Yu, W., Ge, Y., 2016. Hydrological responses to land-use change scenarios under constant and changed climatic conditions. Environ. Manag. 57 (2), 412–431.

Zhang, X., Zhang, L., Zhao, J., Rustomji, P., Hairsine, P., 2008. Responses of streamflow to changes in climate and land use/cover in the Loess Plateau, China. Water Resour. Res. 44 (7). https://doi.org/10.1029/2007WR006711 (n/a-n/a).

Zhang, A., Zheng, C., Wang, S., Yao, Y., 2015. Analysis of streamflow variations in the Heihe River basin, northwest China: trends, abrupt changes, driving factors and ecological influences. J. Hydrol. Reg. Stud. 3, 106–124.

Zheng, H., Zhang, L., Zhu, R., Liu, C., Sato, Y., Fukushima, Y., 2009. Responses of streamflow to climate and land surface change in the headwaters of the Yellow River basin. Water Resour. Res. 45 (7). https://doi.org/10.1029/2007WR006665 (n/a-n/a).

Zhou, F., Xu, Y., Chen, Y., Xu, C.Y., Gao, Y., Du, J., 2013. Hydrological response to urbanization at different spatio-temporal scales simulated by coupling of CLUE-S and the SWAT model in the Yangtze River Delta region. J. Hydrol. 485, 113–125.

Zuo, D., Xu, Z., Yao, W., Jin, S., Xiao, P., Ran, D., 2016. Assessing the effects of changes in land use and climate on runoff and sediment yields from a watershed in the Loess Plateau of China. Sci. Total Environ. 544, 238–250.